Dalton Transactions

PAPER

View Article Online
View Journal | View Issue

Cite this: *Dalton Trans.*, 2014, **43**, 4361

Probing the metallating ability of a polybasic sodium alkylmagnesiate supported by a bulky bis(amido) ligand: deprotomagnesiation reactions of nitrogen-based aromatic substrates†

David R. Armstrong,[a] William Clegg,[b] Alberto Hernán-Gómez,[a] Alan R. Kennedy,[a] Zoe Livingstone,[a] Stuart D. Robertson,[a] Luca Russo[b] and Eva Hevia*[a]

Exploring the reactivity of sodium butylmagnesiate reagent [{Na(THF)$_6$}$^+${(Ph$_2$Si(NAr*)$_2$)Mg(Bu)(THF)}$^-$] (**1**) supported by the bulky chelating silyl(bisamido) ligand {Ph$_2$Si(NAr*)$_2$}$^{2-}$ (Ar* = 2,6-iPr$_2$-C$_6$H$_3$) towards *N*-methylbenzimidazole (**blm^{Me}**), pyrrole and 2,6-diisopropylaniline (NH$_2$Ar*), this study provides new insights into the ability of this bimetallic base to facilitate direct Mg–H exchange reactions as well as to exhibit polybasicity. Thus **1** effectively promotes the deprotomagnesiation of **blm^{Me}** under mild reaction conditions to give the α-metallated intermediate [{Na(THF)$_5$}$_2^+${(Ph$_2$Si(NAr*)$_2$)Mg(blm^{Me}*)}$_2^-$] (**2**) (blm^{Me}* = 2-*N*-methylbenzimidazolyl). Analysis of crystallographic and NMR data of **2** combined with DFT calculations show that the metallated C in the blm^{Me}* ligands possesses a significant carbenic character. Contrasting with previous studies of benzothiazole (**btz**), **1** does not react with an excess of **blm^{Me}** even under forcing refluxing conditions. Contrastingly, the amination reactions of equimolar amounts of **1** with pyrrole and 2,6-diisopropylaniline allowed the isolation of [{(Ph$_2$Si(NAr*)(NHAr*))Mg(NC$_4$H$_4$)$_2$(THF)Na(THF)$_2$}] (**3**) and [{Na(THF)$_6$}$^+${(Ph$_2$Si(NAr*)(NHAr*))Mg(NHAr*)$_2$(THF)}$^-$] (**4**) respectively as crystalline solids. Highlighting the ability of **1** to act as a polybasic reagent, **3** and **4** are formed as the result of the deprotonation of two molecules of the relevant amine *via* its butyl group and one amido arm of the silyl(bisamido) ligand. Similarly, the reactions of **1** with 3 molar equivalents of the relevant amine yielded homoleptic tris(amido) compounds [(THF)$_2$NaMg(NC$_4$H$_4$)$_3$] (**5**) and [{Na(THF)$_6$}$^+${Mg(NHAr*)$_3$}$^-$] (**7**), with the concomitant formation of bis(amine) Ph$_2$Si(NHAr)$_2$, as a result of the complete amination of **1** using its three basic sites. The structures in the solid state of **3** and **4** were elucidated by X-ray crystallography. Despite their similar constitution, these heteroleptic tris(amido)magnesiates adopt contrasting structures, with the former displaying a contacted ion-pair structure, where Na and Mg are connected by two bridging pyrrolyl anions, whereas the latter gives rise to a solvent-separated ion pair motif. To the best of our knowledge **3** represents the first crystallographically characterized magnesium compound containing an anionic non-substituted form of pyrrole. Noticeably, Mg interacts exclusively with the N atoms of the pyrrolyl ligands, forming strong σ-bonds, whereas Na prefers to engage with the π-systems of both NC$_4$-rings.

Received 23rd September 2013,
Accepted 23rd October 2013

DOI: 10.1039/c3dt52639a

www.rsc.org/dalton

Introduction

The synthesis of magnesium compounds supported by sterically demanding ligands, such as β-diketiminates, guanidinates, N-heterocyclic carbenes or bis(amides), is attracting increasing widespread interest.[1] Providing a protective steric shelter, the use of these ligands has been instrumental in recent landmarks in Mg chemistry, which include the isolation of the first stable Mg–Mg bonded compounds,[2] as well as the trapping of novel high nuclearity magnesium-hydride clusters, having important implications as models for hydrogen

[a]*WestCHEM, Department of Pure and Applied Chemistry, University of Strathclyde, Glasgow G1 1XL, UK. E-mail: eva.hevia@strath.ac.uk*
[b]*School of Chemistry, Newcastle University, Newcastle upon Tyne, NE1 7RU, UK*

† Electronic supplementary information (ESI) available: CIF files giving crystallographic results, experimental and computational details and proposed mechanism for the formation of [Na$_2$Mg$_2$(L1)$_2$(THF)$_5$] (Scheme 1)]. CCDC 960101–960103. For ESI and crystallographic data in CIF or other electronic format see DOI: 10.1039/c3dt52639a

storage.[3] Within the context of catalysis, magnesium complexes supported by β-diketiminate ligands have proved to be extremely active single-site initiators for polymerisation of *rac*-lactide[4] as well as efficient precatalysts for intramolecular hydroamination reactions of a wide range of aminoalkenes.[5] Contrastingly, the effects bulky ligands may have on the reactivity/structures of alkali-metal magnesiate compounds remain largely unstudied. This is particularly surprising as members of this mixed-metal family are versatile and efficient polar organometallic reagents, finding extensive applications in many important synthetic transformations, including nucleophilic alkylation, magnesium–halogen exchange or deprotonation (C–H bond breaking) reactions, to name a few.[6] By operating synergistically, alkali-metal magnesiates can exhibit superior chemo- and regioselectivities and/or functional group tolerances to conventional monometallic reagents. Recent breakthroughs in this area include Knochel's turbo Grignard reagents RMgCl·LiCl, whose enhanced nucleophilicity allows direct magnesiation (*via* Mg–halogen exchange reactions) of aromatic molecules with sensitive organic functional groups, without the need for cryogenic conditions,[7] as well as the use of heterobimetallic amides in alkali-metal-mediated magnesiation (AMM*Mg*) processes to facilitate in certain cases the regioselective deprotonation of organic substrates in remote positions, not available using single-metal bases.[8] We recently reported the synthesis of the solvent-separated sodium magnesiate $[\{Na(THF)_6\}^+\{(Ph_2Si(NAr^*)_2)Mg(Bu)(THF)\}^-]$ (**1**) resulting from the reaction of homoleptic $NaMgBu_3$ with the silylbis(amine) precursor $Ph_2Si(NHAr^*)_2$, which contains bulky 2,6-diisopropylphenyl substituents (Ar*).[9] On treatment with benzothiazole (**btz**), **1** is transformed to the complex molecular assembly $[Na_2Mg_2(L1)_2(THF)_5]$, where L1 is a novel trianionic ligand resulting from the deprotonation and coupling of three **btz** molecules, one of which ring opens (Scheme 1; the proposed mechanism for this cascade process involving magnesiation, C–C coupling, ring opening, nucleophilic addition and intramolecular deprotonation is depicted in Scheme S1 in ESI file†). The unique outcome of this activation process contrasts sharply with the straightforward reactivity reported for more conventional organomagnesium reagents such as Hauser bases or Grignard reagents, which can readily deprotonate **btz** at its C2 position in quantitative yields.[10] Our initial studies show that rather than act as a mere spectator, the bis(amido) ligand $\{Ph_2Si(NAr^*)_2\}^{2-}$ plays a prominent role in facilitating this cascade of fast intramolecular reactions, acting as a base through both its amido arms with concomitant formation of bis(amine) $Ph_2Si(NHAr^*)_2$ (Scheme 1).[9] Furthermore, it appears that the deprotonation of the first molecule of **btz**, by the Bu base in **1**, is the rate determining step in the process. Further evidence supporting this proposal has been found by investigating the reactivity of **btz** with β-diketiminate stabilised magnesium reagents, which show that a closely related cascade activation process is also in operation when a kinetically resilient butyl derivative is employed, although in this case the β-diketiminate ligand acts as a steric stabiliser rather than a base.[11]

Stimulated by these intriguing initial findings and aiming to gain a better understanding of the metallating ability of sodium magnesiate **1** and its involvement in the above mentioned **btz** activation process, herein we extend our reactivity studies towards the related 1,3-benzoazole *N*-methylbenzimidazole (**bIm^{Me}**) as well as exploring its amination reactions with the amines pyrrole and 2,6-diisopropylphenylaniline, NH_2Ar^*.

Results and discussion

Direct magnesiation of *N*-methylbenzimidazole

We started our studies by studying the reaction of sodium magnesiate **1** with *N*-methylbenzimidazole **bIm^{Me}** whose hydrogen atom at the C2 position between the N atoms is substantially less acidic than that in benzothiazole (calculated pK_a values, 32.5 for **bIm^{Me}** *vs.* 27.5 for **btz**).[12] The room-temperature 1 : 1 reaction in THF solution afforded a pale green solution which on cooling deposited a crop of yellow crystals of $[\{Na(THF)_5\}_2^+\{(Ph_2Si(NAr^*)_2)Mg(bIm^{Me}*)\}_2^-]$ (**2**) (bIm^{Me}* = 2-*N*-methylbenzimidazolyl) in a 71% isolated yield (Scheme 2).

X-ray crystallographic studies of **2** confirmed that C2-magnesiation of **bIm^{Me}** has taken place, giving rise to a solvent separated ion pair complex containing two sodium cations, each solvated by five THF molecules, and a novel dinuclear dianion comprising two $\{(Ph_2Si(NAr^*)_2)Mg\}$ fragments connected by two bridging *N*-methylbenzimidazolyl bIm^{Me}* ligands. These ligands coordinate in an asymmetric fashion *via* their metallated carbon and one of their N atoms (C1 and N1 in Fig. 1). This distinct bonding mode closes a six-membered {MgCNMgCN} ring, which is fused through each of its Mg

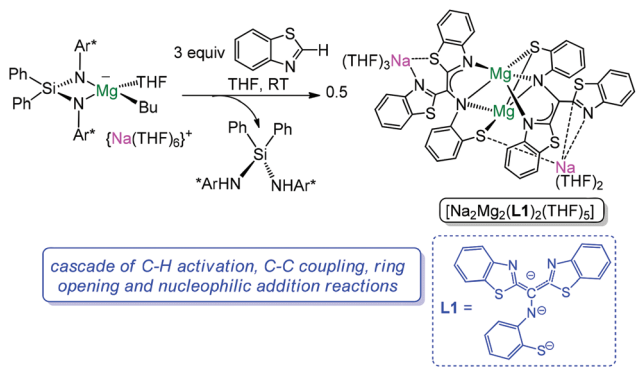

Scheme 1 Magnesium-mediated cascade activation of **btz**.

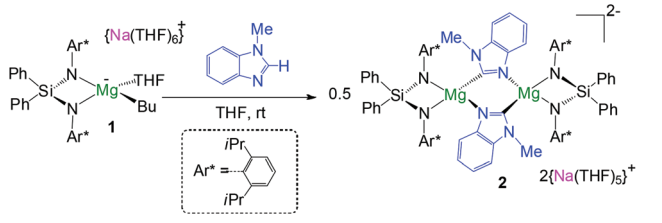

Scheme 2 Direct magnesiation of **bIm^{Me}** using sodium magnesiate **1**.

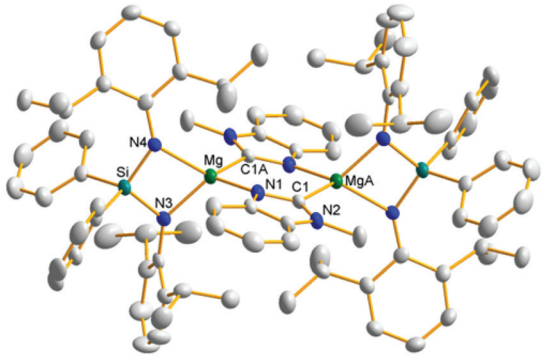

Fig. 1 Structure of the anion of **2** with displacement ellipsoids drawn at the 50% probability level and hydrogen atoms are omitted for clarity. Selected bond lengths (Å) and angles (°): Mg–N1 2.091(2), Mg–C1A 2.233(3), Mg–N3 2.028(2), Mg–N4 2.160(2), C1–N1 1.362(3), C1–N2 1.380(3), N3–Mg–N4 76.74(4), N3–Mg–N1 118.00(9), N1–Mg–C1A 102.91(10), N4–Mg–C1A 124.85(9), N3–Mg–C1A 116.18(10), N4–Mg–N1 118.32(9), Si–N4–Mg 89.54(9), MgA–C1–N2 123.14(18), MgA–C1–N1 129.24(19), N1–C1–N2 106.9(2). The suffix A denotes an inversion-related atom.

vertices to a four-membered {MgNSiN} ring, resulting from the coordination of the bis(amide) ligand to Mg. The distorted tetrahedral geometry of Mg [bond angles ranging from 76.74(4) to 124.85(9)°; mean 109.41°] indicates an approximately orthogonal disposition of this 4-6-4 fused ring system. This structural motif has a strong resemblance with that recently reported for deprotonation of **bIm^{Me}** using a homometallic Mg amido base supported by the β-diketiminate ligand nacnac (nacnac = Ar*NC(Me)CHC(Me)NAr*, Ar* = 2,6-i-Pr$_2$-C$_6$H$_3$) as it also exhibits a dimeric arrangement with a central six-membered ring,[11] although in this case no discussion of its geometrical parameters was possible due to the low precision of the structure. A comparison of Mg–N$_{bis(amido)}$ bond distances in **2** shows a noticeable asymmetry in the coordination of this chelating ligand to the Mg centre [Mg–N4, 2.160(2) Å *vs.* Mg–N3, 2.028(2) Å], which could be attributed to the steric constraints imposed by the rigid tricyclic structure of **2**. Interestingly, it should also be noted that the Mg–N$_{bImMe*}$ bond length in **2** [Mg–N1, 2.091(2) Å] lies in the same range of these Mg–N$_{amido}$ values, and is considerably shorter than that reported in the related Mg complex [(nacnac)Mg(Bu)(bIm^{Me})] [Mg–N1, 2.144(2) Å],[11] where **bIm^{Me}** coordinates as a neutral N-donor to Mg, hinting at the presence of at least some partial negative character of the nitrogen atom. Moreover, despite the sp^2 character of C, the Mg–C bond distance [Mg–C1A, 2.233(3) Å] is distinctly elongated compared to that of the butyl precursor **1** which also contains a similar pseudotetrahedral Mg environment [Mg–C$_{Bu}$, 2.124(3) Å].[9] This, coupled with the subtle but noticeable variation of the N–C bonds of the imidazolyl rings [C1–N1, 1.362(3) Å; C1–N2, 1.380(3) Å] when compared to those of related 5-amino-1-methyl-benzimidazole [1.3785(18) and 1.350(2)][13] suggest that these bridging ligands exhibit a noticeable carbenic character, and therefore **2** can be envisaged as a 1-methyl-3-[magnesium bis(amido)]benzimidazol-2-ylidene dimer. Supporting this interpretation, the Mg–C bond distance in **2** is within the range of other values reported for Mg–N-heterocyclic carbene complexes [ranging from 2.200(2) to 2.288(5) Å].[14] Closely related, seminal studies by Boche *et al.* on the structure of lithiated 1-methyl-4-*tert*-butylimidazole have also established the significant carbenic character of the imidazolyl ligands, by eloquently comparing the structural differences of this compound with those found for imidazole and for the related NHC 1,3-bis(1-adamantyl-imidazol-2-ylidene).[15,16] Interestingly, the coordination flexibility of imidazolyl ligands has recently been highlighted by Hayton *et al.* for the synthesis of bimetallic compounds containing uranyl-nacnac fragments, where the binding modes of these ligands to U (as carbanions or N donors in their carbene resonance form) can be finely controlled by modifying the electronic properties of the accompanying metal.[17] Contrasting with this tunability, computational studies on the tautomerization of free imidazole to its NHC form show that this process is energetically unfavoured, being endothermic by almost 30 kcal mol^{-1}.[18] However, it should be noted that by using a stepwise strategy of sequential deprotonation and electrophilic interception, recent studies in d-block chemistry have revealed the effective transformation of *N*-alkyl imidazoles coordinated to transition metal fragments to N-heterocyclic carbenes.[19]

Solubility in deuterated THF enabled **2** to be characterized in solution using ^{1}H and ^{13}C NMR spectroscopy (see the Experimental section for details). The most informative resonance in the ^{13}C NMR spectrum appears at 194.0 ppm for the C2 carbon of bIm^{Me*} which is significantly downfield compared to the C2 resonance observed in free bIm^{Me} (142.7 ppm) and also noticeably different from that reported for the metallated C of an α-magnesiated *N*-methylindole species (181.1 ppm).[20] Supporting the interpretation of the solid-state studies, reflecting the markedly carbenic character of the bIm^{Me*} ligands in **2**, this chemical shift corresponds more closely to those previously reported for the C$_{carbene}$ in NHC–Mg complexes such as adduct ^{n}Bu$_8$Mg$_4$·2IPr (IPr = 1,3-bis-(2,6-diisopropylphenyl)imidazol-2-ylidene) which resonates at 197.3 ppm.[14f]

Remarkably both ^{1}H and ^{13}C NMR spectra of **2** displayed well resolved signals with no detectable resonances that could be assigned to a ring-open α-(isocyano)methylanilide species, resulting from the cleavage of the C–N$_{Me}$ bond of the bIm^{Me*} groups. This contrasts with previous NMR studies carried out for 2-lithiated-benzimidazole which show the existence of an equilibrium at room temperature between its ring-opened and ring-closed isomers.[21]

To probe the energetics involved in the formation of **2**, theoretical calculations at the DFT level employing the B3LYP method[22] and the 6-311G** basis set were used to model the metallation reaction of **bIm^{Me}** by sodium magnesiate **1** (see ESI† for details), showing that the formation of **2** (modelled as monomer **2A**) is favoured by −13.9 kcal mol^{-1}.[23] This energy gain is even more substantial when considering the dimeric structure exhibited by **2** in the solid state, as the dimerization of **2A** to give dimer **2B** was estimated to be exothermic by −71.4 kcal mol^{-1}.[24]

Comparing the calculated geometrical parameters of **2B** with those determined experimentally from the X-ray crystallographic studies of **2** shows, in general, an excellent agreement (see Table 1 for selected bond distances and angles), with a slight overestimation for the calculated Mg–N1 bond [2.144 Å (calc.) *vs.* 2.091(2) Å (exp)]. Interestingly, when comparing the relative stabilities of the two possible isomers of monomeric **2A**, as an *N*-metallacarbene (**2A$_1$**) or its carbanionic resonance (**2A$_2$**) (Fig. 2), it was found that the former is negligibly more stable (by 1.6 kcal mol^{-1}), which supports previous experimental findings on the bonding flexibility of imidazolyl ligands when coordinated to metal centres. It should be noted that in model **2A$_1$**, the imidazolyl ligand coordinates to magnesium in an η^2-fashion through its C and N atoms, forming a relatively short Mg–N bond with the imidazolyl ligand (2.099 Å), which is comparable with the Mg–N bond distance found experimentally in **2** (2.091(2) Å) as well as a Mg–C contact (2.163 Å) which is slightly elongated compared to that calculated for **2A$_2$** (2.133 Å) where Mg binds solely to the carbon of the bIm^{Me*} ligand. Related η^2-(N,C)-coordination has been experimentally observed for the structures of lithiated 1-methyl-4-*tert*-butylimidazole and benzothiazole.[15] Dimerization of **2A$_1$** to form **2B** results in the cleavage of this Mg–C bond to generate a new bond with the Mg centre of a neighbouring monomer. Consistent with its carbene resonance form, the difference between the calculated N–C bond distances of the imidazolyl ring in **2A$_1$** is significantly more subtle [$\Delta(d_{C-N}-d_{CNMe})$ = 0.022 Å] than that computed for **2A$_2$** [$\Delta(d_{C-N}-d_{CNMe})$ = 0.067 Å], supporting a more localised N–C=N$_{Me}$ bonding scenario for the latter, similar to that calculated for the parent *N*-methylbenzimidazole (see ESI† for details, $\Delta(d_{C-N}-d_{CNMe})$ = 0.073 Å). Furthermore, a comparison of these theoretical values with that found experimentally in **2** [$\Delta(d_{C1-N2}-d_{C1N2})$ = 0.018 Å] offers further support to the carbenic character attributed to its bIm^{Me*} bridges on the basis of the X-ray crystallographic and NMR spectroscopic studies.

Table 1 Comparison of selected calculated bond distances (Å) and angles (°) for model **2B** with those from the X-ray crystallographic data of **2**

	2	**2B**
Mg–N1	2.091(2)	2.144
Mg–C1A	2.233(3)	2.270
Mg–N3	2.028(3)	2.082
Mg–N4	2.160(2)	2.210
C1–N1	1.362(2)	1.357
C1–N2	1.380(3)	1.384
N1–Mg–C1A	102.9(10)	100.8
N3–C1–N1	118.00(9)	107.6
N3–Mg–N4	76.74(4)	76.4

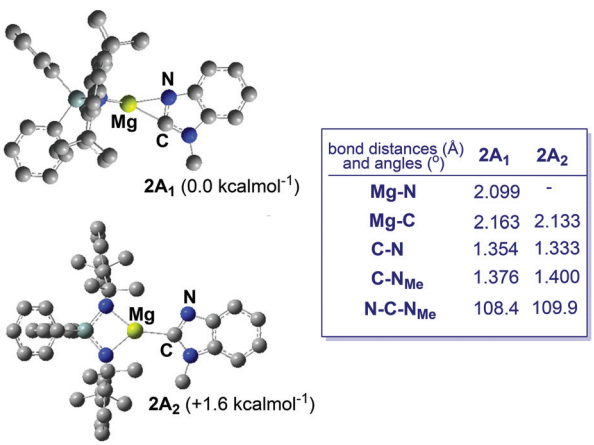

Fig. 2 Modelled structures and selected calculated bond distances and angles for the anionic moieties of monomeric **2A$_1$** and **2A$_2$**.

The regioselective C2-magnesiation of **bIm^{Me}** by **1** differs significantly from the reactivity previously reported for related 1,3-benzoazole, **btz**, where the three potential basic arms of **1** react with the heterocycle, even when 1 : 1 mixtures of these starting materials are employed, to form the complicated activation product [$Na_2Mg_2L_2(THF)_5$] depicted in Scheme 1.[9] Furthermore, no further metallation was observed when isolated crystals of **2** were confronted with a 2 molar excess of **bIm^{Me}**, even when the mixture was heated at 65 °C over a 5 hour period, evidencing the resilience of the amido groups of the {$Ph_2Si(NAr*)_2$} ligand to promote the deprotonation of **bIm^{Me}**. Notwithstanding, considering that for the activation of **btz** the rate-determining step appears to be its metallation by the butyl group **1**, **2** can be envisaged as an indirect model for the first intermediate involved in this cascade activation process, which in turn reacts with two further equivalents of **btz** to form the final product (Scheme 1 and S1 in ESI†). Interestingly, it should also be noted that the exclusive alkyl basicity displayed by **1** diverges from the reactivity reported for related homometallic magnesium β-diketiminate [(nacnac)Mg(Bu)(THF)], which fails to metallate, even under refluxing conditions, leading to the isolation of a simple coordination product, resulting from substitution of the THF molecule coordinated to Mg by a molecule of **bIm^{Me}**, acting as a neutral 2 electron-donor.[11] The enhanced metallating ability of **1** over neutral [(nacnac)Mg(Bu)(THF)] can be rationalised in terms of its bimetallic anionic ate constitution, which enables the activation of an otherwise kinetically retarded butyl group.[25] Illustrating this activating effect, Mulvey has reported the high-yielding room temperature α-magnesiation of *N*-methylindole using sodium tetrabutylmagnesiate [$(TMEDA)_2NaMgBu_4$], where each Bu group reacts with one equivalent of the substrate, whereas $MgBu_2$ on its own fails to deprotonate this same heterocycle.[20]

Extension to pyrrole and 2,6-diisopropylaniline: polybasic behaviour of magnesiate base

In order to explore the possibility of **1** acting as a polybasic reagent, we next turned our attention to the heterocyclic amine pyrrole. Its N–*H* group has a pK_a value of 23 making it significantly more acidic than the C_2–*H* of **bIm^{Me}**.[26] Surprisingly, we found that even when equimolar amounts of this substrate and mixed-metal base **1** were employed, compound [{(Ph_2Si-(NAr*)(NHAr*))$Mg(NC_4H_4)_2(THF)Na(THF)_2$}] (**3**), resulting from

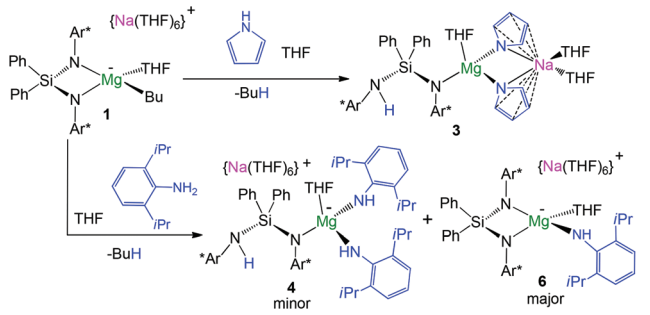

Scheme 3 Amination reactions of **1** with pyrrole and 2,6-diisopropylaniline.

the deprotonation of two molecules of pyrrole, *via* the butyl group and amido arm of the bis(amido) ligand present in **1**, was obtained in a 17% isolated yield (Scheme 3) as a crystalline product. Compound **3** was characterized by multinuclear ^{1}H and ^{13}C NMR spectroscopy and its structure elucidated by X-ray crystallography, which confirmed its bimetallic constitutions (see the Experimental section and ESI† for details). Interestingly, when the rational synthesis of **3** was attempted by reacting butylmagnesiate **1** with two molar equivalents of pyrrole at room temperature, compound **3** was obtained as a crystalline solid along with variable amounts of tris(amido) $[(THF)_2NaMg(NC_4H_4)_3]$ (**5**), with the later resulting from the complete amination of **1** involving its three potentially basic arms. The formation of this compound can be significantly minimised by carrying out the addition of the amine at 0 °C, which affords **3** in an improved 57% yield (see the Experimental section for details).[27] Tris(pyrrolyl)magnesiate **5** was characterised by ^{1}H and ^{13}C NMR spectroscopy and could be prepared and isolated in a 49% yield by treating **1** with 3 equivalents of pyrrole (see Table S2 and ESI† for details).[28]

Highlighting the complexity of these amination reactions, extending these studies to the primary amine 2,6-diisopropylaniline, led to the formation of complicated mixtures of products. Thus, the reaction of equimolar amounts of this aniline and **1** deposited a few colourless crystals of the double amination product $[\{Na(THF)_6\}^+\{(Ph_2Si(NAr^*)(NHAr^*))Mg(NHAr^*)_2(THF)\}^-]$ (**4**),[29] the structure of which was determined in the solid state by X-ray crystallography (Fig. 4). However, ^{1}H NMR analysis of the solution filtrate showed that the major product of the reaction was $[\{Na(THF)_6\}^+\{(Ph_2Si(NAr^*)_2)Mg(NHAr^*)(THF)\}^-]$ (**6**), resulting from the reaction of the butyl group of **1** with the amine (Scheme 3). Contrastingly, ^{1}H NMR monitoring of the reaction of **1** with two molar equivalents of the aniline afforded a complex mixture of the three possible amination products **4**, **6** and tris(anilido) $[\{Na(THF)_6\}^+\{Mg(NHAr^*)_3\}^-]$ (**7**) in a 1 : 2.1 : 1.1 ratio,[30] whereas when three equivalents of NH_2Ar were employed, compound **1** was quantitatively converted into tris(anilido) **7** and bis(amine) $Ph_2Si(NHAr_2)$.[31]

Despite their similar tris(amido) constitution, sodium magnesiates **3** and **4** exhibit remarkably different structures in the solid state (Fig. 3 and 4, respectively). Although in both cases Mg displays a similar coordination environment, adopting a distorted four-coordinate tetrahedral geometry (mean angle

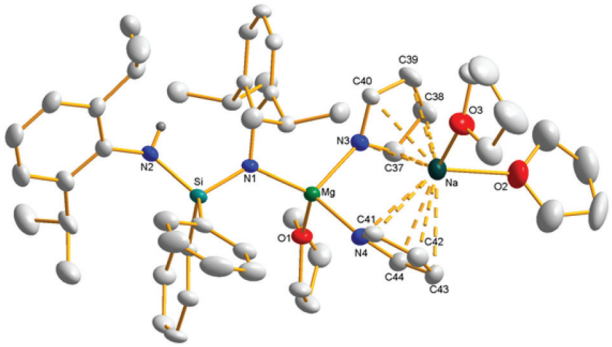

Fig. 3 Molecular structure of **3** with displacement ellipsoids drawn at the 50% probability level and hydrogen atoms (except NH) and minor disorder components in THF ligand are omitted for clarity. Selected bond lengths (Å) and angles (°): Na–O3 2.265(2), Na–O2 2.294(16), Na–N3 2.635(2), Na–N4 2.796(2), Na–C37 2.721(3), Na–C38 3.002(3), Na–C39 3.066(3), Na–C40 2.837(3), Na–C41 3.016(3), Na–C42 3.137(3), Na–C43 2.960(3), Na–C44 2.729(3), Mg–O1 2.033(17), Mg–N1 2.015(18), Mg–N3 2.0514(19), Mg–N4 2.060(2), N1–Mg–O1 115.23(7), N1–Mg–N3 114.99(8), O1–Mg–N3 99.54(7), N1–Mg–N4 123.27(8), O1–Mg–N4 100.61(8), N3–Mg–N4 99.46(8).

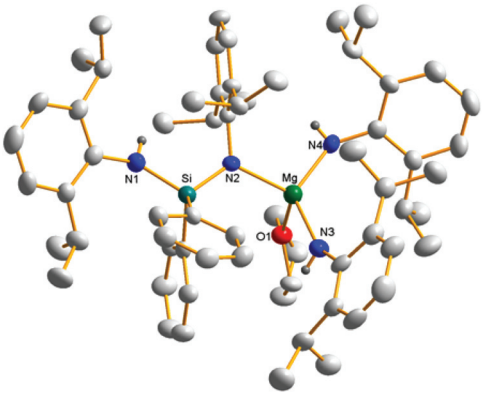

Fig. 4 Structure of anion moiety in **4** with displacement ellipsoids drawn at the 50% probability level and hydrogen atoms (except NHs) are omitted for clarity.

around Mg 108.85° for **3** and 108.88° for **4**), being bound by two newly formed amide ligands as well as terminal amido(silyl)amine $\{Ph_2Si(NAr^*)(NHAr^*)\}$ and a solvating molecule of THF, **3** displays a contacted-ion pair structure, where Na and Mg are connected by two pyrrolyl bridges, whereas in **4**, Na is solvated by six molecules of THF, giving rise to a solvent-separated ion pair motif. In both cases the new amine NHAr* group, generated by protonation of the chelating bis(amido) ligand of **1**, does not interact with the Mg centre, which instead prefers coordination by a molecule of the donor solvent THF. This coordination preference contrasts with that found in the lithium dimer $[\{Ph_2Si(2,6\text{-}Et_2C_6H_3NH)(2,6\text{-}Et_2C_6H_3NLi)\}_2]$ which contains a similar amido(silyl)amine, bonding in a chelating fashion *via* its two N atoms to Li.[32] Unfortunately, the structure of **4** was derived from a twinned and weakly diffracting crystal sample and also features considerable disorder with respect to the THF groups. Thus, despite several attempts at data collection, the final model is

of a relatively low precision, which prevents discussion of any geometrical parameters, although its connectivity is definite.[33]

The structure of **3** is notable for having distinct bonding preferences of Na and Mg to the pyrrolyl anions. Thus, while Mg coordinates exclusively in a σ-manner forming relatively short (strong) Mg–N bonds [Mg–N3, 2.0514(19) Å and Mg–N4 2.060(2) Å], Na engages with the π-systems of both pyrrolyl NC_4-rings. The pattern of the bond distances in these Na···π-face interactions denotes η^5-NC_4 coordination, with noticeably shorter Na···N contacts [Na–N3, 2.635(2) Na–N4, 2.796(2) Å] than the remaining Na···C [ranging from 2.721(3) to 3.066(3) Å and from 2.729(3) to 3.137(3) Å for each NC_4 ring], which can be attributed to the more electron-rich character of the amido N atoms. Furthermore, in order to maximize this Na···π-surface bonding, both pyrrolyl rings are tilted towards the Na cation, as evidenced by the narrow N3–Mg–N4 bond angle [99.46(8)°]. Reflecting the isoelectronic and close structural relationship between pyrrolyl and cyclopentadienyl (C_5H_5, Cp) rings, the η^5-NC_4 π-bonding present in **3** bears a strong resemblance to that found in other NaCp species which have been structurally elucidated, as for example polymeric $[\{Na(DME)(\eta^5\text{-}C_5H_5\}_\infty]$ (DME = 1,2-dimethoxyether).[34] Interestingly, a similar σ/π bonding distinction to that observed in **3** has been recently described by Mulvey *et al.* for a series of sodium-zincate pyrrolyl complexes.[35] Contrastingly, this earlier study reveals that, in the homometallic sodium derivative $[\{PMDETA)Na(NC_4H_4)\}_2]$, the Na cation interacts only with the N atoms of the pyrrolyl units, avoiding any possible π-contact with the aromatic ring,[35] which suggests that for heterobimetallic **3**, the metal–N σ bonding preference of the NC_4H_4 is dictated by the stronger Lewis acidity of Mg in comparison to Na. As far as we can ascertain, **3** represents the first crystallographically characterized magnesium compound containing an anionic non-substituted form of pyrrole.[36]

The ^{1}H NMR spectrum of **3** in deuterated benzene solution showed a broad singlet at 4.10 ppm for the N*H* group and two diagnostic multiplets for the CH groups of the ^{i}Pr substituents of the amido(silyl)amine $\{Ph_2Si(NAr^*)(NHAr^*)\}$ ligand at 4.48 and 2.79 ppm which can be assigned to its amido NAr* and amine NHAr* arms, respectively.[37] Reflecting the increased negative charge of the N centres of the pyrrolyl ligands in **3** in comparison with the N–H unit in pyrrole, the signals attributed to the α-positions of the heterocycle in both ^{1}H and ^{13}C NMR spectra appear significantly more shielded (at 6.50 and 136.6 ppm, respectively) than to those found for free pyrrole (at 6.37 and 117.5 ppm, respectively).[38] This effect is even more pronounced for tris(amido) $[(THF)_2NaMg(NC_4H_4)_3]$ (**5**) whose α-H′s appear at 7.69 ppm in its ^{1}H NMR spectrum (Table S2, ESI†).

Collectively, these findings from the amination reactions of **1** demonstrate the ability of the bis(amido) ligand $\{Ph_2Si(NAr)_2\}$ present within sodium magnesiate **1** to participate in Mg–H exchange processes, converting, in this case, the N–H bonds of either pyrrole or 2,6-diisopropylaniline, into new Mg–N bonds. Furthermore, the fact that these conversions take place even with equimolar amounts of **1** and the relevant amine shows that depending on the activation level of the substrate employed, **1** can execute polybasic behaviour even under substoichiometric conditions, using its amido arms. Thus rather than act as a spectator, providing a steric shield to the Mg centre, this bis(amido) ligand can also play a prominent role in facilitating the metallation of more than one molecule of the substrate by the bimetallic base, which in some cases can lead to a Mg centre coordinating simultaneously to several sensitive anions, facilitating activation processes like the one depicted in Scheme 1 for **btz**.

Conclusions

This study demonstrates that sodium magnesiate **1**, which is supported by the bulky chelating bis(amido) ligand $\{Ph_2Si(NAr^*)_2\}$, can effectively promote direct Mg–H exchange reactions. Thus, the metallation products of its reaction with **bIm^{Me}** and the amines pyrrole and 2,6-diisopropylaniline, **2**, **3** and **4**, respectively, have been isolated and structurally elucidated. Contrasting with our previous reactivity studies with the related 1,3 benzoazole **btz**, **1** acts exclusively as a butyl base towards **bIm^{Me}**, facilitating its selective C2-metallation affording **2**. X-ray crystallographic studies of **2** established its dimeric constitution, containing an unusual dinuclear magnesiate dianion, where the benzimidazolyl ligands coordinate asymmetrically through their metallated C and N atoms to the Mg centres. Analysis of its crystallographic and NMR spectroscopic data coupled with DFT studies revealed that the Mg–*C* atoms of the bIm^{Me*} fragments of **2** display a significant carbenic character. Reactivity studies show that even under forcing refluxing conditions and using an excess of **bIm^{Me}**, the potentially basic arms of the bis(amido) ligand in **1** are unable to deprotonate this N-heterocyclic molecule. Notwithstanding, **2** can be envisaged as a model for the first intermediate proposed to be involved in the cascade activation of **btz** mediated by **1**, where the rate-determining step appears to be the deprotonation of **btz** by the butyl group of **1**. Establishing the ability of **1** to execute polybasicity, its reactions with equimolar amounts of the amines pyrrole and 2,6-diisopropylaniline led to the isolation of the double amination products **3** and **4** as crystalline solids. Varying the stoichiometry of these reactions has shown that complete amination of **1**, using its butyl group and two amido arms of the bulky chelating ligand, can be accomplished using 3 equivalents of the relevant amine, allowing the isolation of homoleptic tris(amido)magnesiates **5** and **7**.

Collectively these findings shed new light on the reactivity of **1**, unveiling its potential to execute selective deprotomagnesiation reaction, as well as providing new mechanistic insights into its role in the cascade activation of **btz**, where **1** uses all three of its basic arms to formally deprotonate three molecules of this heterocycle.

Experimental section

Full experimental and computational details are included in the ESI.† CCDC 960101–960103 contain the supplementary crystallographic data of this paper.

Synthesis of $[\{Na(THF)_5\}_2^+\{(Ph_2Si(NAr^*)_2)Mg(bIm^{Me^*})\}_2^-]$ (2)

1-Methylbenzimidazole (0.13 g, 1 mmol) was added to a solution of isolated crystals of **1** (1.14 g, 1 mmol) in THF (3 ml) affording a pale green solution that was stirred at room temperature for 2 hours. Hexane (5 ml) was added and the resulting solution was transferred to a freezer (−30 °C). After 48 hours, a crop of yellow crystals was isolated (0.76 g, 71%). ^{1}H NMR (d_8-THF, 298 K) δ 7.76 [d, 4H, Ph], 6.99 [m, 6H, Ph], 6.95 [m, 1H, MeBIm*], 6.94 [m, 1H, bIm^{Me^*}], 6.88 [d, 4H, Ar*], 6.59 [t, 2H, Ar*], 6.33 [m, 1H, bIm^{Me^*}], 6.12 [t, 1H, bIm^{Me^*}], 4.10 [m, 4H, C*H*, ^{i}Pr, Ar*], 3.61 [m, 20H, OCH_2, THF], 3.51 [s, 3H, CH_3, bIm^{Me^*}], 1.76 [m, 20H, CH_2, THF], 0.78 [d, 24H, CH_3, ^{i}Pr, Ar*]. ^{13}C{^{1}H} NMR (d_8-THF, 298 K) δ 194.0 [*C*–Mg], 155.9, 155.3, 148.5, 145.4, 143.4 [$C_{quaternary}$, Ph, Ar* and bIm^{Me^*}], 136.9 [*C*H, Ph], 127.6 [*C*H, Ph], 127.4 [*C*H, Ph], 123.8 [*C*H, Ar*], 123.1, 121.0, 120.6 [*C*H, bIm^{Me^*}], 117.5 [*C*H, Ar*], 116.8 [*C*H, bIm^{Me^*}], 68.2 [O–*C*H_2, THF], 34.6 [*C*H_3, bIm^{Me^*}], 29.3 [*C*H, ^{i}Pr, Ar*], 27.3 [*C*H_3, ^{i}Pr, Ar*], 26.3 [CH_2, THF].

Synthesis of $[\{(Ph_2Si(NAr^*)(NHAr^*))Mg(NC_4H_4)_2(THF)Na(THF)_2\}]$ (3)

Pyrrole (0.07 ml, 1 mmol) was added to a solution of sodium magnesiate 1 (1.14 g, 1 mmol) in hexane (5 ml), affording a suspension which was stirred at room temperature for 30 minutes. THF (4 ml) was introduced and the suspension gently heated until all the solid was dissolved affording a pale yellow solution. This solution was transferred to the freezer (−30 °C) and colourless crystals were obtained after 4 days, which were isolated by filtration and transferred to the glove box (isolated yield 0.155 g, 17%, note that employing this stoichiometry, the maximum possible yield for **3**, with respect to **1** is 50%). This yield could be improved to 57% (0.530 g) when two equivalents (0.14 ml, 2 mmol) of pyrrole were employed, carrying out the amination reaction at 0 °C to minimize the formation of tris(amido)magnesiate $[(THF)_2NaMg(NC_4H_4)_3\}]$ (**5**).[34] ^{1}H (C_6D_6, 298 K) δ 8.17 [d, 4H, Ph], 7.27–7.11 [12H, m, Ph and Ar*], 6.50 [s, α-C*H*, $MgNC_4H_4$], 6.13 [s, 4H, β-C*H*, $MgNC_4H_4$], 4.48 [m, 2H, C*H*, ^{i}Pr, NAr*], 4.10 [s, 1H, N*H*], 3.35 [m, 24H, OC*H*2, THF], 2.79 [m, 2H, C*H*, ^{i}Pr, NHAr*], 1.34 [d, 6H, CH_3, ^{i}Pr, NAr*], 1.27 [m, 24H, CH_2, THF], 1.06 [d, 6H, CH_3, ^{i}Pr, NAr*], 0.92 [d, 12H, CH_3, ^{i}Pr, NHAr*]. ^{13}C{^{1}H} NMR (C_6D_6, 298 K) δ149.9, 146.5, 142.9, 142.5, 139.0 [$C_{quaternary}$, Ph and Ar*], 136.6 [*C*H, Ph], 128.5 [α-*C*H, $MgNC_4H_4$], 127.3 [*C*H, Ph], 127.1 [*C*H, Ph], 124.5, 123.6, 121.3, 120.5 [*C*H, Ar*], 107.0 [β-*C*H, $MgNC_4H_4$], 68.2 [O–*C*H_2, THF], 28.2 [*C*H, ^{i}Pr, NAr*], 27.7 [*C*H, ^{i}Pr, NHAr*] 25.8 [*C*H, ^{i}Pr, NAr*], 25.3 [CH_2, THF], 24.23 [*C*H_3, iPr, NHAr*], 23.6 [*C*H_3, ^{i}Pr, NAr*].

Acknowledgements

We thank the EPSRC (equipment funding to W. C.), the University of Strathclyde (studentship to Z. L.), the Royal Society (University Research Fellowship to E. H.), and the European Research Council (ERC) for the generous sponsorship of this research.

Notes and references

1 For selected references see: (*a*) L. T. Evans, M. P. Coles, F. G. N. Cloke and P. B. Hitchcock, *J. Organomet. Chem.*, 2007, **692**, 2548; (*b*) M. Arrowsmith, M. S. Hill, D. MacDougall and M. F. Mahon, *Angew. Chem., Int. Ed.*, 2009, **48**, 4013; (*c*) S. J. Bonyhady, D. Collis, G. Frenking, N. Holzmann, C. Jones and A. Stasch, *Nat. Chem.*, 2010, **2**, 865; (*d*) B. M. Day, N. E. Mansfield, M. P. Coles and P. B. Hitchcock, *Chem. Commun.*, 2011, **47**, 4995; (*e*) M. Arrowsmith, M. R. Crimmin, M. S. Hill, S. L. Lomas, D. J. MacDougall and M. F. Mahon, *Organometallics*, 2013, **32**, 4961.

2 (*a*) S. P. Green, C. Jones and A. Stasch, *Science*, 2007, **318**, 1754; (*b*) A. Stasch and C. Jones, *Dalton Trans.*, 2011, **40**, 5659.

3 (*a*) S. Harder, J. Spielmann, J. Intemann and H. Bandmann, *Angew. Chem., Int. Ed.*, 2011, **50**, 4156; (*b*) J. Intemann, J. Spielmann, P. Sirsch and S. Harder, *Chem.–Eur. J.*, 2013, **19**, 8478.

4 For selected references see: (*a*) M. H. Chisholm, J. C. Huffman and K. Phomphrai, *J. Chem. Soc., Dalton Trans.*, 2001, 222; (*b*) B. M. Chamberlain, M. Cheng, D. R. Moore, T. M. Ovitt, E. B. Lobkovsky and G. W. Coates, *J. Am. Chem. Soc.*, 2001, **123**, 3229; (*c*) M. H. Chisholm, J. C. Gallucci and K. Phomphrai, *Inorg. Chem.*, 2002, **41**, 2785; (*d*) A. P. Dove, V. C. Gibson, E. L. Marshall, A. J. P. White and D. J. Williams, *Dalton Trans.*, 2004, 570; (*e*) F. Drouin, T. J. J. Whitehorne and F. Schaper, *Dalton Trans.*, 2011, **40**, 1396.

5 (*a*) M. R. Crimmin, M. Arrowsmith, A. G. M. Barrett, I. J. Casely, M. S. Hill and P. A. Procopiou, *J. Am. Chem. Soc.*, 2009, **131**, 9670; (*b*) A. G. M. Barrett, I. J. Casely, M. R. Crimmin, M. S. Hill, J. R. Lachs, M. F. Mahon and P. A. Procopiou, *Inorg. Chem.*, 2009, **48**, 4445; (*c*) A. G. M. Barrett, M. R. Crimmin, M. S. Hill and P. A. Procopiou, *Proc. R. Soc. London, Ser. A*, 2010, **466**, 927.

6 For reviews in the area see: (*a*) R. E. Mulvey, *Organometallics*, 2006, **25**, 1060; (*b*) R. E. Mulvey, F. Mongin, M. Uchiyama and Y. Kondo, *Angew. Chem., Int. Ed.*, 2007, **46**, 3802; (*c*) R. E. Mulvey, *Acc. Chem. Res.*, 2009, **42**, 743; (*d*) B. Haag, M. Mosrin, H. Ila, V. Malakhov and P. Knochel, *Angew. Chem., Int. Ed.*, 2011, **50**, 9794; (*e*) R. E. Mulvey, *Dalton Trans.*, 2013, **42**, 6676; (*f*) A. Harrison-Marchand and F. Mongin, *Chem. Rev.*, 2013, **113**, 7470; (*g*) A. Harrison-Marchand and F. Mongin, *Chem. Rev.*, 2013, **113**, 7563.

7 A. Krasovskiy and P. Knochel, *Angew. Chem., Int. Ed.*, 2004, **43**, 3333.

8 (*a*) P. C. Andrikopoulos, D. R. Armstrong, W. Clegg, C. J. Gilfillan, E. Hevia, A. R. Kennedy, R. E. Mulvey, C. T. O'Hara, J. A. Parkinson and D. M. Tooke, *J. Am. Chem. Soc.*, 2004, **126**, 116121; (*b*) P. C. Andrikopoulos, D. R. Armstrong, D. V. Graham, E. Hevia, A. R. Kennedy, R. E. Mulvey, C. T. O'Hara and C. Talmard, *Angew. Chem., Int. Ed.*, 2005, **44**, 3459; (*c*) E. Hevia, G. W. Honeyman,

A. R. Kennedy, R. E. Mulvey and D. C. Sherrington, *Angew. Chem., Int. Ed.*, 2005, **44**, 68; (*d*) P. C. Andrikopoulos, D. R. Armstrong, E. Hevia, A. R. Kennedy and R. E. Mulvey, *Organometallics*, 2006, **25**, 2415.

9 V. L. Blair, W. Clegg, A. R. Kennedy, Z. Livingstone, L. Russo and E. Hevia, *Angew. Chem., Int. Ed.*, 2011, **50**, 9857.

10 (*a*) M. Shilai, Y. Kondo and T. Sakamoto, *J. Chem. Soc., Perkin Trans. 1*, 2001, 442; (*b*) A. Krasovskiy, V. Krasovskaya and P. Knochel, *Angew. Chem., Int. Ed.*, 2006, **45**, 2958.

11 S. E. Baillie, V. L. Blair, T. D. Bradley, W. Clegg, J. Cowan, R. W. Harrington, A. Hernán-Gómez, A. R. Kennedy, Z. Livingstone and E. Hevia, *Chem. Sci.*, 2013, **4**, 1895.

12 K. Shen, Y. Fu, J. N. Li, L. Liu and Q. X. Guo, *Tetrahedron*, 2007, **63**, 1568.

13 J. Lokaj, V. Kettmann, V. Milata and T. Solčan, *Acta Crystallogr., Sect. E: Struct. Rep. Online*, 2009, **65**, o1788.

14 For references of structurally defined magnesium compounds containing NHC ligands see: (*a*) A. J. Arduengo III, H. R. V. Dias, F. Davidson and R. L. Harlow, *J. Organomet. Chem.*, 1993, **462**, 13; (*b*) D. Zhang and H. Kawaguchi, *Organometallics*, 2006, **25**, 5506; (*c*) P. L. Arnold, I. J. Casely, Z. R. Turner, R. Bellabarba and R. B. Tooze, *Dalton Trans.*, 2009, 7236; (*d*) M. Arrowsmith, M. S. Hill, D. J. MacDougall and M. F. Mahon, *Angew. Chem., Int. Ed.*, 2009, **48**, 4013; (*e*) A. R. Kennedy, R. E. Mulvey and S. D. Robertson, *Dalton Trans.*, 2010, **39**, 9091; (*f*) A. R. Kennedy, R. E. Mulvey and S. D. Robertson, *Dalton Trans.*, 2010, **39**, 9091; (*g*) A. R. Kennedy, J. Klett, R. E. Mulvey and S. D. Robertson, *Eur. J. Inorg. Chem.*, 2011, 4675.

15 C. Hilf, F. Bosold, K. Harms, J. C. Lohrenz, M. Marsch, M. Schimeczek and G. Boche, *Chem. Ber./Recl.*, 1997, **130**, 1201.

16 It should be noted that, contrasting with the relatively simple dimeric structure of **2**, this compound exhibits a more complex supramolecular assembly, containing 16 Li atoms and 8 imidazolyl fragments combined with 2 oxo and 4 alkoxo ligands. These oxygen-based anions have been formed as a consequence of the degradation of the ethereal solvents employed by methyl lithium, which is the organometallic reagent used for the deprotonation of 1-methyl-4-*tert*-butylimidazole.

17 M. F. Schettini, G. Wu and T. W. Hayton, *Chem. Commun.*, 2012, **48**, 1484.

18 G. A. McGibbon, C. Heinemann, D. J. Lavorato and H. Schwarz, *Angew. Chem., Int. Ed.*, 1997, **36**, 478.

19 (*a*) J. Ruiz and B. F. Perandones, *J. Am. Chem. Soc.*, 2007, **129**, 9298; (*b*) M. A. Huertos, J. Perez, L. Riera, J. Diaz and R. Lopez, *Angew. Chem., Int. Ed.*, 2010, **49**, 6409; (*c*) M. Brill, J. Diaz, M. A. Huertos, R. Lopez, J. Perez and L. Riera, *Chem.–Eur. J.*, 2011, **17**, 8584; (*d*) C. H. Hsieh, R. Pulukkody and M. Y. Darensbourg, *Chem. Commun.*, 2013, **49**, 9326.

20 B. Conway, E. Hevia, A. R. Kennedy and R. E. Mulvey, *Chem. Commun.*, 2007, 2864.

21 C. Hilf, F. Bosold, K. Harms, M. Marsch and G. Boche, *Chem. Ber./Recl.*, 1997, **130**, 1213.

22 (*a*) A. D. Becke, *J. Chem. Phys.*, 1993, **98**, 5648; (*b*) C. Lee, W. Yang and R. G. Parr, *Phys. Rev. B: Condens. Matter*, 1988, **37**, 785; (*c*) S. H. Vosko, L. Wilk and M. Nusair, *Can. J. Phys.*, 1980, **58**, 1200; (*d*) P. J. Stephens, F. J. Devlin, C. F. Chabalowski and M. J. Frisch, *J. Phys. Chem.*, 1994, **98**, 11623.

23 The reaction of **1** and **bIm^{Me}** to give monomeric **2A** was modelled considering only the anionic magnesiate moieties of **1** (**1A**) and **2A**, see ESI† for details.

24 This value was estimated using the resulting point energies of placing the Na cations 15 Å away from their anionic counterparts, using the Mg atoms as the origin. This approximation was made in order to simulate the solvent-separated ion-pair structure found experimentally for **2**.

25 For a related study comparing the kinetic reactivity of Mg–C bonds *vs.* Mg–N bonds for the deprotonative metalation of anisole using potassium magnesiate bases see: W. Clegg, B. Conway, P. Garcia-Alvarez, A. R. Kennedy, R. E. Mulvey, L. Russo, J. Sassmannshausen and T. Tuttle, *Chem.–Eur. J.*, 2009, **15**, 10702.

26 pK_a value determined in DMSO solution, for details see: F. G. Bordwell, *Acc. Chem. Res.*, 1988, **21**, 456.

27 See ESI† for synthetic and spectroscopic details of tris(amido)magnesiate **5**. It should be noted that even under these reaction conditions, ^{1}H NMR analysis of crystalline samples of the crystalline product showed the presence of **5** in an approximately 7% ratio.

28 Compound **5** was isolated as a crystalline solid along with trace amounts of bis(amine) $Ph_2Si(NHAr^*)_2$ which is the byproduct resulting from the reaction of **1** with 3 molar equivalents of pyrrole. ^{1}H NMR integration indicated that this impurity is present in an approximately 5% ratio.

29 Despite numerous attempts, compound **4** could not be prepared as a pure compound. ^{1}H NMR analysis of crystalline samples isolated from the reaction of **1** with variable amounts of 2,6-diisopropylaniline shows the presence of **4** as a minor product along with variable amounts of **6**, **7**, $Ph_2Si(NHAr^*)_2$ and in some cases unreacted **1**. Although these spectra are quite complicated, with significant overlapping of most of the signals, the resonances for the *para*-H of the NHAr* ligands are well resolved (see Fig. S1, ESI†) and their integration can be used to estimate the ratio of products **4**, **6** and **7** present in solution.

30 Using 1.5 equivalents of NH_2Ar^* afforded a mixture of products where the single-amination product **6** was the major species present in solution (the **4** : **6** : **7** ratio was found to be 1.1 : 5 : 1, see Fig. S1, ESI†).

31 $[\{Na(THF)_6\}^+\{Mg(NHAr^*)_3\}^-]$ (**7**) was isolated as a colourless oil, see ESI† for synthesis and spectroscopic characterization details.

32 N. Palanisami and R. Murugavel, *J. Organomet. Chem.*, 2006, **691**, 3260.

33 For other related structurally elucidated magnesium amides containing 2,6-diisopropylanilide see: (*a*) M. M. Olmstead,

W. J. Grigsby, D. R. Chacon, T. Hascall and P. P. Power, *Inorg. Chim. Acta*, 1996, **251**, 273; (*b*) A. Xia, M. J. Heeg and C. H. Winter, *Organometallics*, 2002, **21**, 4717; (*c*) E. Hevia, A. R. Kennedy, R. E. Mulvey and S. Weatherstone, *Angew. Chem., Int. Ed.*, 2004, **43**, 1709; (*d*) B. Conway, E. Hevia, A. R. Kennedy, R. E. Mulvey and S. Weatherstone, *Dalton Trans.*, 2005, 1532.

34 M. L. Cole, C. Jones and P. C. Junk, *Dalton Trans.*, 2002, 896.

35 J. A. Garden, A. R. Kennedy, R. E. Mulvey and S. D. Robertson, *Dalton Trans.*, 2011, **40**, 11945.

36 For other examples of substituted variants see: (*a*) A. Xia, M. J. Heeg and C. H. Winter, *Organometallics*, 2002, **21**, 4718; (*b*) T. K. Panda, K. Yamamoto, K. Yamamoto, H. Kaneko, Y. Yang, H. Tsurugi and K. Mashima, *Organometallics*, 2012, **31**, 2268.

37 A comparison of the chemical shifts observed for the C*H* resonance of the ^{i}Pr groups in the ^{1}H NMR spectra in C_6D_6 of bis(amine) precursor $\{Ph_2Si(NHAr^*)_2\}$ and the bis(amide) ligand in **1** shows a similar trend. Thus, a multiplet at 3.38 ppm is observed for the NHAr* fragment, which is significantly more shielded than that found for the NAr*amide groups (at 3.98 ppm).

38 See the Experimental section and Table S2 in ESI† for details. It should be noted that this trend in the chemical shifts of pyrrolyl anions has also been reported in sodium-zincate chemistry, see ref. 35.